

Study on behavior of T-section modular composite profiled beams

Soo-Hyun Ryu

Department of Architectural, Sahm-Yook University, Seoul, Korea

(Received March 10, 2010, Accepted August 25, 2010)

Abstract. In this study, specimens were made with profile thicknesses and shear reinforcement as parameters. The bending and shear behavior were checked, and comparative analysis was conducted of the results and the theoretical values in order to see the applicability of T-section Modular Composite Profiled Beams (TMPB). In TMPB, the profiles of formwork functions play a structural role resisting the load. Also, the module concept, which is introduced into TMPB, has advantages: it can be mass-produced in a factory, it is lighter than an existing H-beam, it can be fabricated on the spot, and its section size is freely adjustable. The T1 specimens exhibited ductile behavior, where the whole section displayed strain corresponding to yielding strain at least without separation between modules. They also exhibited maximum strength similar to the theoretical values even if shear reinforcement was not applied, due to the marginal difference between shear strength and maximum bending moment of the concrete section. A slip between modules was incurred by shear failure of the bolts in all specimens, excluding the T1 specimen, and therefore bending moment could not be fully displayed.

Keywords: T-section; modular; composite; profiled; slip; shear reinforcement.

1. Introduction

Despite advantages of superior strength, high toughness, less self weight, convenient construction, material uniformity, etc., a steel structure has inherent problems including fire resistance, deflection, and vibration. Also, a reinforced concrete structure has advantages of durability, plasticity, sound insulation, seismic performance, etc. However, it also has disadvantages of economic efficiency from formwork use, heavy self weight, dry shrinkage, creep, etc.

Therefore, research and development on the composite structure, which has the merits of both a steel structure and a reinforced concrete structure, is being actively conducted. For composite beams, which are being currently developed and used, where typically concrete slabs and steel beams using a deck plate on the top are composed of stud bolts, the concept is merely composed of concrete slabs on the upper part with steel beams on the lower part, thus a question about their efficiency is being raised. Therefore, studies on composite beams have been attempted, in which reinforced concrete beams are applied having merits including vibration and deflection, instead of steel beams and are reinforced with various materials. Existing methods include the joining of a side plate onto the constructed RC beam with a bolt (Oehlers *et al.* 1997, 2000) or adhesive (Oehlers *et al.* 2000) and reinforcement with FRP

* Corresponding author, Mr., E-mail: ryu129@hanmail.net

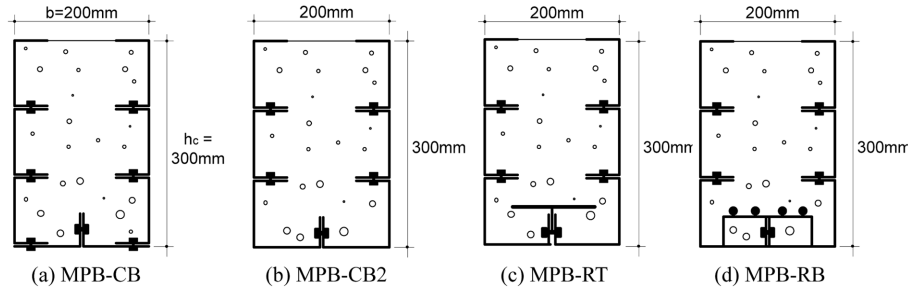


Fig. 1 Specimens section of existing study

(Minglan *et al.* 2004) and CFRP (Bencardino *et al.* 2002, Kim *et al.* 2004). Among these, the profile-based method has characteristics including an alternative to formwork and increased structural performance. The author therefore suggested the side and lower modules of the C-type and Lip-type in a previous study (Ahn *et al.* 2007) as shown in Fig. 1(a), and conducted an analytical study with the parameters of bolt connection and tension plate reinforcement. Also, a new module was suggested as shown in Fig. 1(b), and reinforcing bars and T section steel were applied with bending reinforcement parameters to propose an appropriate bending reinforcement method as shown in Figs. 1(c), (d) (Ahn *et al.* 2008). As a result of this study, the improved and reinforced cross section showed the increased flexural strength, and when a theoretical value was calculated with design compressive stress of the concrete (f_{ck}) and minimum yield stress (f_y) of the steel, most experimental values exceeded the theoretical value. However, previous studies have been limited to rectangular sections; therefore, buckling of the steel of the compressive part had an effect on experimental results. Also, in terms of the beam, once shear strength (except for bending) acts simultaneously, shear strength may greatly influence the beam according to the shear span ratio or the level of load. Therefore, bending behavior as well as shear behavior needs to be understood. Therefore, TMPB, which extended the previously proposed rectangular module profile beams (MPB) to a T-shaped beam, was applied and a theoretical equation was suggested in this study. In addition, an experiment was conducted with parameters of the thickness of profile and the type of stirrup used, and the general shear reinforcement form of reinforced concrete beam. Also, comparative analysis was conducted of experimental results and theoretical values to determine the applicability of TMPB.

2. Flexural strength of T-section modular composite profiled beams

The TMPB was analyzed by referring to the equation suggested by Oehlers's theoretical method (1993, 1994). Flexural strength is calculated by rigid plastic analysis of the application of yielding stress to the whole section of steel and $0.85f_{ck}$ to the compression section of concrete. Unless the steel section exhibits fully plastic behavior, the bending moment is calculated using strain for each part. The basic assumption applied to calculate the plastic bending moment was as follows: Stress of $0.85f_{ck}$ is equally distributed in the compression area of concrete, and the height of the compression area is calculated according to a ratio of the bond strength. The tensile strength of concrete is 0. For steel, it is specified that uniform yielding stress (f_y) is distributed with compression at the top and tensile strength at the bottom centered on the plastic neutral axis.

2.1 Full shear connection analysis (FSC)

2.1.1 Case of plastic neutral axis located in slab ($P_1 + P_2 \leq 0.85f_{ck} \cdot \beta_1 \cdot t_s \cdot B$)

When concrete and steel behave in a body, as shown in Fig. 2 (b), concrete controls the compressive strength and transforms the bond of tensile strength into an equilibrium state, which can be expressed by Eq. (1) as follows

$$C_c = 0.85f_{ck} \cdot \beta_1 \cdot N_c \cdot B = P_b \tag{1}$$

- Here, C_c : Compressive strength of concrete
- f_{ck} : Design compressive stress of the concrete
- β_1 : $0.85-0.007(f_{ck}-28)$
- N_c : Plastic neutral axis of concrete
- P_b : Maximum bond strength between concrete and steel
- B : Width of slab

N_c is expressed by Eq. (2) as follows

$$N_c = \frac{P_b}{0.85f_{ck} \cdot \beta_1 \cdot B} \tag{2}$$

Considering the general force equilibrium of concrete and steel, the bond strength acting on the tension part of the concrete shall act on the compression part of the steel element to establish force equilibrium. This is as shown in Fig. 2 (c), and the force equilibrium is expressed by Eq. (3) as follows.

$$P_1 + P_2 = P_b \tag{3}$$

- Here, P_1, P_2 : Plastic tensile strength of upper & lower module ($P_1 = A_1 \cdot f_{yp}$)
- A_1, A_2 : Area of upper & lower module
- f_{yp} : Yielding stress of the profile

The neutral axis N_c can be obtained upon full shear connection by substituting the result of Eq. (3)

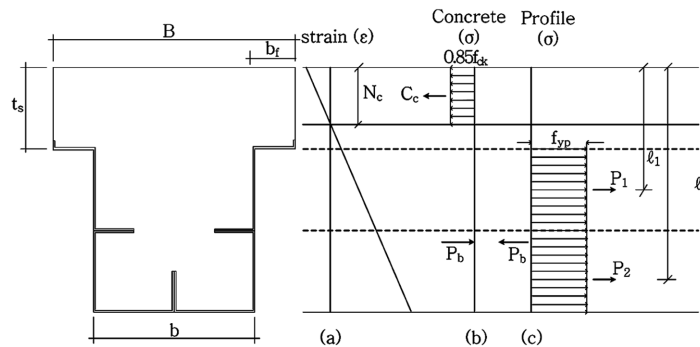


Fig. 2 Stress & Strain (in the case of plastic neutral axis located in the slab)

into Eq. (2). The plastic bending moment (M_p) of TMPB is a moment at the end of the compression part of the section, which is as shown in Eq. (4). The bond strength is then the strength at the same positions acting in opposite directions; therefore the contribution to bending moment is 0.

$$M_p = P_1 \cdot l_1 + P_2 \cdot l_2 - \frac{0.85f_{ck} \cdot \beta_1^2 \cdot N_c^2 \cdot B}{2} \tag{4}$$

Here, l_1, l_2 : Distance from the top compression fiber to the centroid of each module

2.1.2 Case of plastic neutral axis located at upper steel flange

$$(0.85f_{ck} \cdot \beta_1 \cdot t_s \cdot B \leq P_1 + P_2 \leq 0.85f_{ck} \cdot \beta_1 \cdot t_s \cdot B + 4f_{yp} t_p b_f)$$

When concrete and steel behave in a body, as shown in Fig. 3 (b), concrete reaches equilibrium by compressive force, and bond strength reaches equilibrium by tensile strength, as shown in Eq. (5)

$$C_c = 0.85f_{ck}(\beta_1 \cdot N_c \cdot b + 2b_f \cdot \beta_1 \cdot t_s) = P_b \tag{5}$$

- Here, b : Width of concrete beam
- t_s : Thickness of concrete slab
- b_f : Push out Width of concrete flange

N_c can be expressed by Eq. (6) as follows.

$$N_c = \frac{P_b}{0.85f_{ck} \cdot \beta_1 \cdot b} - \frac{2b_f \cdot \beta_1 \cdot t_s}{\beta_1 \cdot b} \tag{6}$$

Force equilibrium in steel elements is as shown in Fig. 3(c). Transforming the force equilibrium involves adding each f_{yp} to the compression part and tensile part of the upper N_p as is shown in Fig. 3(d). The force equilibrium of steel is arranged into Eq. (7) by applying transformed strength as shown in Fig. 3(d).

$$P_1 + P_2 = 2f_{yp} \cdot 2b_f \cdot (N_p - t_s) + P_b \tag{7}$$

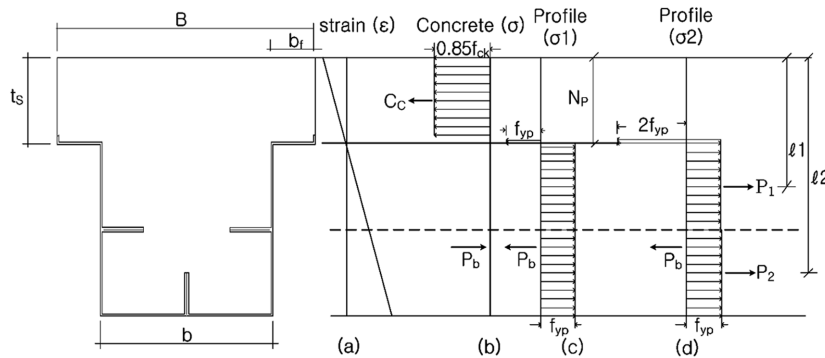


Fig. 3 Stress & Strain (in the case of plastic neutral axis located in the upper flange)

Here, N_p = Plastic neutral axis of profiles

Eq. (7) is arranged in terms of N_p into Eq. (8) as follows

$$N_p = \frac{P_1 + P_2 - P_b}{4f_{yp} \cdot b_f} + t_s \quad (8)$$

Since the full shear connection N_p is equal to N_c , so P_b is calculated using Eq.(6) as equal to Eq.(8), and P_b is used to calculate the neutral axis N_p , N_c . The plastic bending moment M_p is calculated as shown in Eq. (9) as follows using the moment to the end of the compression part.

$$M_p = P_1 \cdot l_1 + P_2 \cdot l_2 - 2f_{yp} \cdot 2b_f \cdot (N_p - t_s) \cdot \left(t_s + \frac{N_p - t_s}{2} \right) - \frac{0.85f_{ck} \cdot \beta_1^2 \cdot N_c^2 \cdot b}{2} \quad (9)$$

2.1.3 Case of plastic neutral axis located in web ($P_1 + P_2 \geq 0.85f_{ck} \cdot \beta_1 \cdot t_s \cdot B + 4f_{yp} \cdot t_p \cdot b_f$)

The equation of equilibrium for concrete elements, when a plastic neutral axis is positioned at the web, is identical to Eq. (5), and the equation to calculate a neutral axis N_c is identical to Eq. (6).

Force equilibrium in steel elements is as shown in Fig. 4(c). Transforming the force equilibrium by adding each f_y to the compression part and the tensile part of upper N_p is as shown in Fig. 4(d). The force equilibrium of steel is arranged into Eq. (10) by applying the transformed strength as shown in Fig. 4(d).

$$P_1 + P_2 = 4f_{yp} \cdot t_p \cdot (N_p - t_s) + 4f_{yp} \cdot t_p \cdot b_f + P_b \quad (10)$$

Here, t_p = Thickness of profile

Eq. (10) is arranged in terms of N_p , as shown in Eq. (11) as follows

$$N_p = \frac{P_1 + P_2 - P_b - 4f_{yp} \cdot t_p \cdot b_f}{4f_{yp} \cdot t_p} + t_s \quad (11)$$

Since it is a full shear connection, N_p is equal to N_c , so P_b is calculated using Eq.(6) as equal to Eq.(11), and using P_b to calculate the neutral axis N_p , N_c . The plastic bending moment M_p is calculated

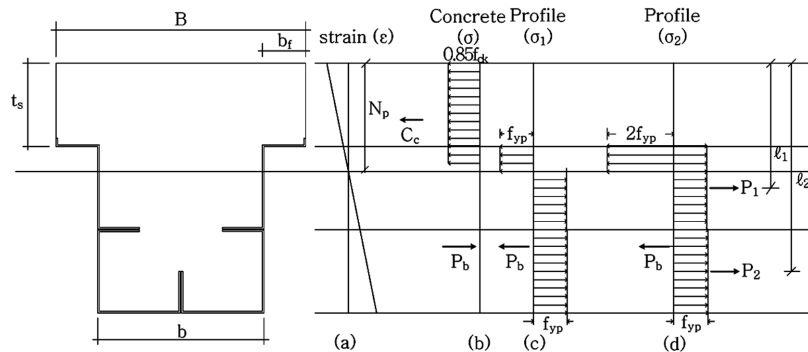


Fig. 4 Stress & Strain (in the case of plastic neutral axis located in the web)

as shown in Eq. (12) as follows using moment to the end of the compression part

$$M_p = P_1 \cdot l_1 + P_2 \cdot l_2 - 2 \cdot 2f_{yp} \cdot t_p \cdot (N_p - t_s) \cdot \left(t_s + \frac{N_p - t_s}{2} \right) - 2 \cdot 2f_{yp} \cdot b_f \cdot t_p \cdot t_s - \frac{0.85f_{ck} \cdot \beta_1^2 \cdot N_c^2 \cdot b}{2} - \frac{0.85f_{ck} \cdot 2b_f \cdot t_s^2}{2} \quad (12)$$

2.2 Partial shear connection analysis (PSC)

2.2.1 Partial shear connection with plastic behavior

This is the case of strain distribution as shown in the form of Fig. 5 (c). Bond strength is calculated as shown in Eq. (13) by multiplying a partial shear connection ratio by P_b in the case of full shear connection. A partial shear connection ratio is calculated by reference to Fig. 5 (c) and (d).

$$(P_b)_{PSC} = Shear \cdot connection \cdot ratio \times (P_b)_{FSC} = X\% \times P_1 + Y\% \times P_2 \quad (13)$$

Here, X%, Y% : Shear connection ratio of upper and lower module, respectively

Since the neutral axis of concrete and steel is not consistent with a slip, the neutral axis of concrete N_c is calculated with Eq.(2) by substituting the result of Eq.(13) into Eq.(3).

By referring to Fig. 5(e), plastic bending moment (M_p) is calculated by multiplying bending moment by the tensile strength of the profile corresponding to the non-slipped amount, and bending moment by compressive strength of concrete, and bending moment by each profile corresponding to the slipped amount, which is as shown in Eq.(14).

$$(M_p)_{PSC} = X\% \cdot P_1 l_1' + Y\% \cdot P_2 l_2' - \frac{0.85f_{ck} \cdot \beta_1^2 \cdot N_c^2 \cdot B}{2} + \sum M_m \quad (14)$$

Here, M_m : Bending moment of each module in portion of slip ratio

2.2.2 Partial shear connection with elasto-plastic behavior

This is the case of strain distribution of steel as shown in the form of Fig. 5 (f). Bond strength is calculated as shown in Eq. (15) as follows.

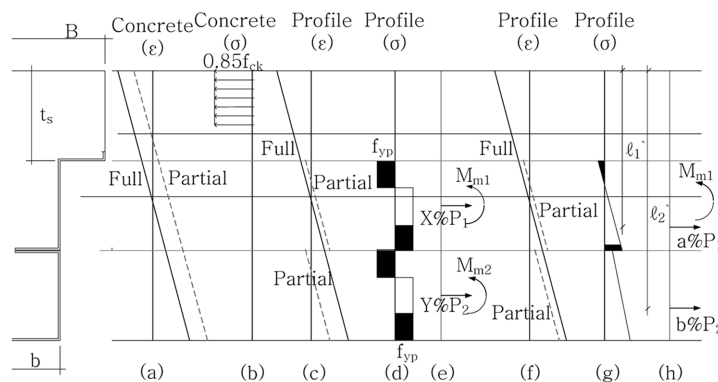


Fig. 5 Stress & Strain (in the case of partial shear connection)

$$(P_b)_{PSC} = a\% \times P_1 + b\% \times P_2 \tag{15}$$

Here a%, b% : Non slip tensile strength ratio of each module (non slip tensile strength/plastic tensile strength) a, b decision made by steel strain curve

By referring to Figs. 5(f), (g), and (h), the bending moment is calculated by multiplying the bending moment by the tensile strength of the profile, the bending moment by the compressive strength of concrete, and the bending moment by each profile, which is as shown in Eq. (16). Since the neutral axis of concrete and steel is not consistent by a slip, the neutral axis N_c of concrete is calculated with Eq. (2) by substituting the result of Eq.(15) into Eq.(3).

$$(M_p)_{PSC} = a\%P_1l_1' + b\%P_2l_2' - \frac{0.85f_{ck}\beta_1^2N_c^2B}{2} + \sum M_m \tag{16}$$

Here l_1' , l_2' : Distance from the top compression fiber to the centroid of each non slip tensile strength

3. Test specimens and material property

3.1 Test specimens

A detailed sectional view of the specimens to investigate the behavior of TMPB is as shown in Fig. 6.

Fig. 6 is a sectional view of the specimen with width, height and length of the beam constant and thickness of the steel varying. For the connection between modules, bolts of 8 mm diameter and 25 mm length were arranged at intervals of 200 mm, and for connection between flange concrete and upper modules, bolts of 8 mm diameter and 75 mm length were arranged at intervals of 200 mm. For stirrup, they were placed onto TS 2, 3, and 4 specimens using D10, D13, and D16 respectively at intervals of 200 mm. Details of specimens by experimental parameters are shown in Table 1. Views of the construction of the specimen are shown in Fig. 7.

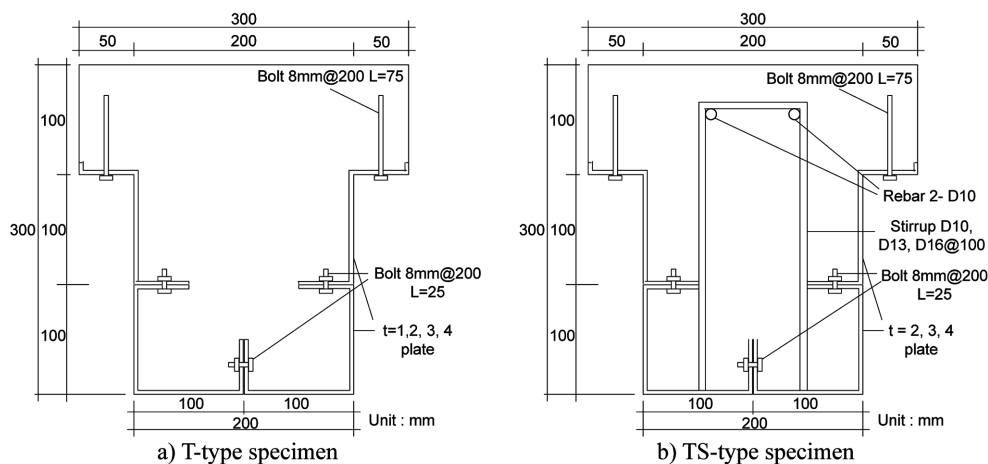


Fig. 6 Section of specimens

Table 1 Detail of specimens

Specimen	Thickness of plate(mm)	Stirrup	Bolt space	Rebar
T1	1	-	200	-
T2	2	-	200	-
T3	3	-	200	-
T4	4	-	200	-
TS2	2	D10@100	200	2-D10
TS3	3	D13@100	200	2-D10
TS4	4	D16@100	200	2-D10

T : T-section, TS : T-section with stirrup



Fig. 7 Specimen details

3.2 Loading and measurement method

For specimen loading, as shown in Fig. 8, two-point loading was given using 490kN UTM (universal test machine). As shown in Fig. 8, each LVDT was installed at both the left and right sides of the central bottom to measure deflection. For strain gauges, concrete was adhered at 4 spots in total of the central top, and the top, middle, and bottom of the side of the beam. Steel was adhered at 6 spots of the top, middle and bottom at the sides of the upper module and lower module, as well as the soffits of the upper flange and lower module. To examine shear behavior of the specimen, a 3-axis rosette gauge was adhered at the center of the upper module, which was 300mm inside the spot, to measure shear strain.

3.3 Material property

3.3.1 Concrete

The design compressive stress of the concrete used in this test was 21 MPa and the concrete was

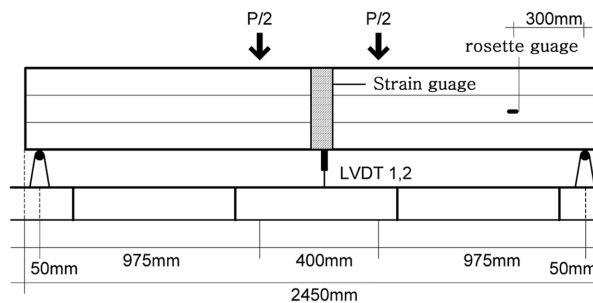


Fig. 8 Position of measurement

Table 2 Concrete mixing ratio

Design stress (MPa)	W/C(%)	Slump(mm)	Unit of aggregate (kg/m ³)			
			W	C	S	G
21	52	150	144	337	931	879

W : Water, C : Cement, S : Fine Aggregate, G : Coarse Aggregate

Table 3 Test results of profile sheet & deformed bar

Specimen	f_{yc}	f_u	E	ϵ_y	f_y / f_u	Elongation Ratio(%)
1 mm	312.0	388.6	185678	1937	0.80	36.4
2 mm	361.7	393.1	191094	1895	0.89	34.4
3 mm	355.1	393.2	189218	1963	0.90	35.2
4 mm	345.1	448.5	196248	2398	0.77	31.4
D10	552.6	677.4	200382	3435	0.82	20.6
D13	528.8	623.5	210315	3491	0.85	21.3
D16	552.6	691.8	201644	3247	0.82	21.4

f_{yc} : Experimental yielding stress(MPa), f_u :Tensile stress(MPa), E: Young's modulus(MPa), ϵ_y :Yielding strain(10^{-6})

cured after on-site placement. Concrete cylinder specimens made in compliance with KS F 2403 were cured under the same condition as the beams, and the compressive stress of the concrete was 21.73 MPa after testing.

3.3.2 Profile sheet and deformed bar

The two specimens were made with the following thicknesses and diameters.

4. Test result and analysis

4.1 Failure shape

The T1 specimen failed due to the development of a diagonal tension crack after the upper concrete underwent compressive failure, as shown in Fig. 9 (a). For other T-type specimens, separation between modules became more severe before it reached the maximum load, and as shown in Fig. 9 (b), with increased deflection of the beam from maximum strength, a diagonal tension crack occurred toward the lower support part from the loading point of the upper left or right. This crack gradually increased, resulting in failure. This condition led to ductile declination from the maximum load. For the TS-type specimens, which underwent shear reinforcement, as shown in Figs. 9 (c) and (d), contrary to T specimens, all specimens failed due to more severe separation between modules and gradually reduced strength after the onset of compression failure at the upper concrete on the beam center. In contrast to T specimens, a diagonal tension crack did not occur; otherwise it did occur after more severe separation between modules from the maximum load. Also, compared to T specimens, the side of the profile displayed larger strain distribution, with superior performance in TS specimens to T specimens in terms of ductility.

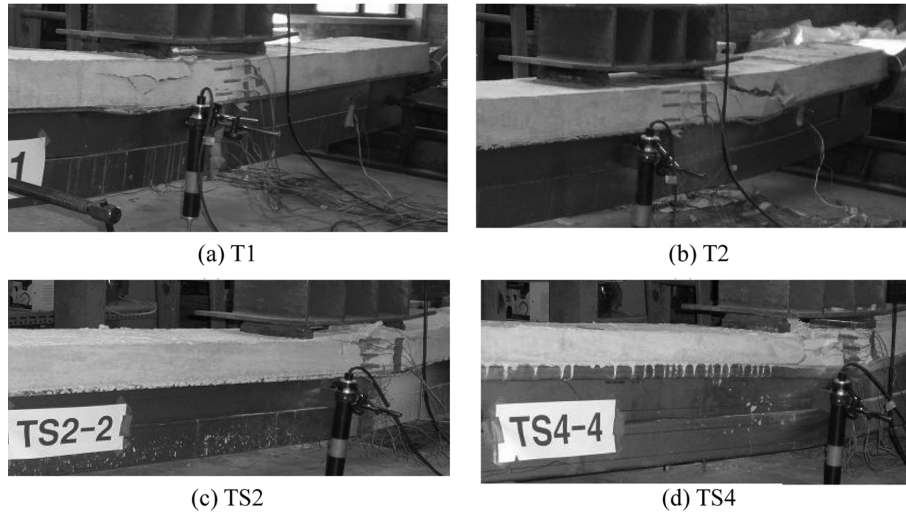


Fig. 9 Failure shape

4.2 Load-deflection and load-strain curves

4.2.1 Load-center deflection

Fig. 10 shows each load-deflection curve for T and TS specimens. The T1 specimen displayed a trend of flexural failure, and load gradually decreased by a slip between modules from the maximum load. The T2 specimen displayed sharply decreased strength from the maximum load, and the T3 and T4 specimens were maintaining initial stiffness but reached maximum strength with sharply decreased stiffness at about 80% of the maximum load. Sharply decreased load appeared thereafter without a plastic plateau.

For the TS specimens, all specimens did not display sharply reduced stiffness by the maximum load, compared to T specimens. After the maximum load, a plastic plateau did not appear, and accordingly deflection increased gently as the load was decreased. It is deemed that this resulted from reduced

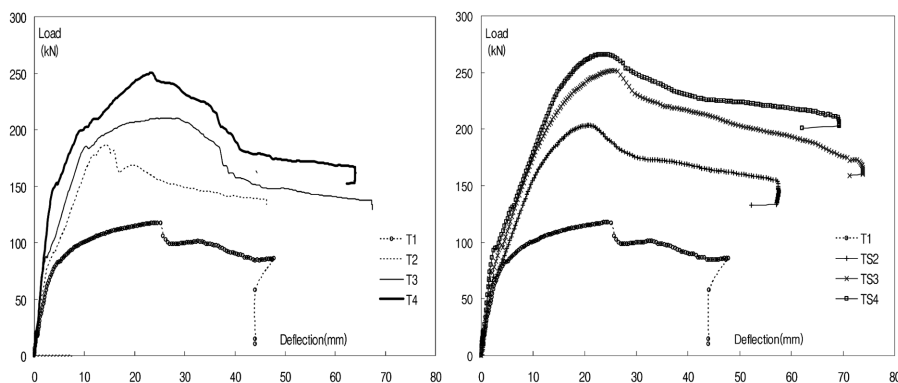


Fig. 10 Load-mid span deflection curves

strength due to a more severe separation between modules. It was found that compared to T specimens, the decrease in stiffness tended to be gentle and stable at initial stiffness and by the maximum load thereafter in TS specimens.

4.2.2 Strain of stirrup and shear strain of side module

Fig. 11(a) shows a load-strain curve of the stirrup. The stirrup of the TS2 specimen displayed a strain of 800×10^{-6} or more, but other specimens showed a strain of 200×10^{-6} or less. Considering that the span of the specimens is identical, it can be found that a smaller steel thickness renders a relatively higher burden to shear. As shown in Fig. 7, a rosette gauge (triaxial gauge) was installed at the center of the upper module 300mm from the end of the specimen to measure the 3-way strain and to calculate maximum shear strain. In Figs. 11 (b), (c) and (d), maximum shear strain is shown per specimen.

The TS specimens with stirrups showed a shear strain of about 400×10^{-6} , while the T specimens without stirrup exhibited maximum shear strain of 600×10^{-6} or more at the maximum load, which indicates that the T specimens had at least 50% higher shear strain than the TS specimens at the maximum load. For the TS specimens, shear strain continued to increase after the maximum load, showing a proportional relation between beam deflection and shear strain. Therefore, it is considered that the bending capacity of the side profile is influenced by shear reinforcement.

4.3 Analysis and discussion

4.3.1 Comparison of test result of maximum load with theoretical load

A comparison between first theoretical maximum load (P_{mt1}) in the case of full shear connection

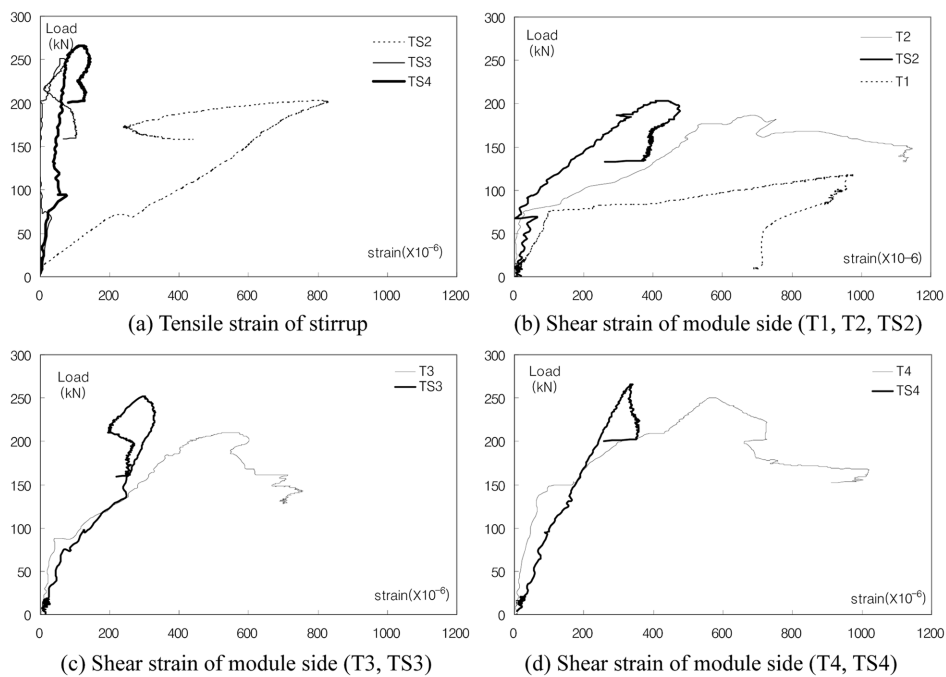


Fig. 11 Strain of stirrup and shear strain of module side

Table 4 Comparison of experimental maximum load with theoretical load

Specimen	P_{me} (kN)	P_{mt1} (kN)	P_{me} / P_{mt1}	P_{mt2} (kN)	P_{me} / P_{mt2}
T1	117.50	119.30	0.98	94.16	1.25
T2	186.49	229.64	0.81	179.69	1.04
T3	210.41	299.93	0.70	217.27	0.97
T4	250.39	348.14	0.72	264.90	0.95
TS2	206.35	229.64	0.90	179.69	1.15
TS3	251.66	299.93	0.84	217.27	1.16
TS4	265.87	348.14	0.76	264.90	1.00

using experimental yielding stress (f_{ye}) and experimental loads (P_{me}) is as shown in Table 4. The actual behavior of specimens can be seen as shown in Fig. 13, and a proper theoretical value can be found by matching the pertinent strain pattern shown in section 2 Flexural strength of T-section Modular Composite profiled Beams. In the T1 specimen, a slip between modules occurred with a ratio of 0.98 between experimental load and theoretical load. However, this is mostly accounted for by plastic behavior, and it is deemed that fully plastic behavior would be possible if a slip would be minimized by improvement in the connection method. The ratios of theoretical maximum load to experimental load were 0.90, 0.84 and 0.76 in the TS2, TS3 and TS4 specimens, respectively, that underwent shear reinforcement, which were found to be higher than the non-reinforced T2, T3 and T4 specimens that were 0.81, 0.70 and 0.72, respectively. Thus after shear reinforcement, the bending capacity of the side profile with less burden of shear strength was found to be improved. The second theoretical maximum load (P_{mt2}) of specimens was replaced by minimum yielding stress f_y instead of experimental yielding stress (f_{ye}) to calculate and compare it with experimental loads (P_{me}), and comparison data are shown in table 4. Comparing results indicates that P_{me} / P_{mt2} exceeded 1.0 except for T3 0.97, and T4 0.95. Therefore suitable shear reinforcing TMPB in the case where f_y is applied instead of f_{ye} , which exceeded the theoretical plastic bending moment (M_p).

4.3.2 Initial stiffness and ductility

The calculation method of yielding load that applies to steel-concrete composite beams is as shown in Fig. 12. The deflection of the point where a horizontal line extending the maximum strength (P_{max}) and

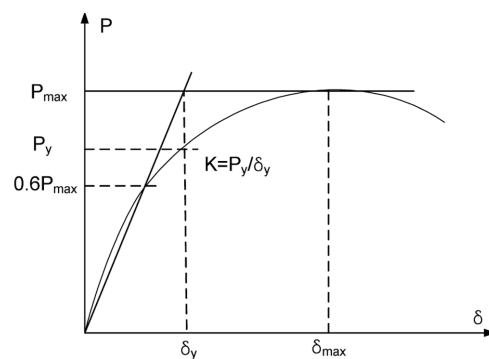


Fig. 12 Yielding load of steel-concrete composite beams

Table 5 Summary of test results

Specimen	Yielding strength			Maximum strength		$\frac{P_{me}}{P_y}$	$\frac{\delta_{max}}{\delta_y}$
	P_y (kN)	δ_y (mm)	Initial stiffness (kN/mm)	P_{me} (kN)	δ_{max} (mm)		
T1	85.06	5.56	15.30	117.50	24.51	1.38	4.41
T2	167.48	10.57	15.84	186.49	14.12	1.11	1.34
T3	174.44	9.00	19.38	210.41	28.67	1.21	3.19
T4	195.90	8.59	22.81	250.39	23.35	1.28	2.72
TS2	172.74	12.25	14.10	203.35	21.14	1.18	1.73
TS3	208.25	13.74	15.16	251.66	25.83	1.21	1.88
TS4	228.34	14.30	15.97	265.87	23.82	1.16	1.67

an extension of stiffness equivalent to 60% of maximum strength on the load-deflection curve meet is the yielding deflection (δ_y). The load at the point where yielding deflection is vertically extended to meet the load-deflection curve is the yielding load (P_y). The experimental result of yielding load, initial stiffness, strength ratio, and deflection ratio are as shown in Table 5. Initial stiffness is defined as a ratio of yielding load to yielding deflection, and a yielding ratio is defined as a ratio of maximum load to yielding load. A deflecting ratio is defined as a ratio of maximum deflection to yielding deflection, representing ductile capacity. The specimens except T3 and T4 represented about 15kN/mm of initial stiffness, and minimal increased stiffness was shown due to steel thickness, but the difference was negligible.

The experiment showed that the strength ratio was 1.3 for the T1 specimen and about 1.2 for other specimens, indicating that the difference in strength ratio was definitely differentiated, which is deemed attributable to the failure of other specimens in fully plastic behavior according to a slip between modules etc. The deflection ratio was found to be superior in the T1 specimen showing fully plastic behavior to other specimens, and a poor deflection ratio was shown in the T2 specimen because a sharp failure occurred without reduced stiffness.

4.3.3 Analysis on strain by position of the strain gauge

The load-strain distribution at the sides of the concrete and profile is as shown in Fig. 13. The longitudinal axis is in the sectional position, the shaded part from the upper end up to the 100mm gauge position is concrete and the remainder is steel, while the lateral axis indicates strain. Each line is a strain curve at a load level divided into the following 4 phases; 30%, 70% of the maximum load, the maximum load, and strength decreased by 80% after the maximum load. Separation between the upper and lower modules in the T1 specimen was not apparent up to the maximum load, and did appear thereafter, though it was more satisfactory compared to other specimens. In the T2 specimen, separation between modules occurred but no compression area occurred at the bottom before it reached the maximum load, and it became more severe after the maximum load and compression area occurred at the top of the lower module. In the T3 and T4 specimens, separation between modules became more severe before it reached the maximum load, and the compression area appeared at the top of the lower module.

More strain was apparent in the TS specimens that underwent shear reinforcement compared to the T specimens, which indicates that shear strength shared by shear reinforcement induced increased bending moment. The concrete top of the TS2 and TS3 specimens underwent compression failure at

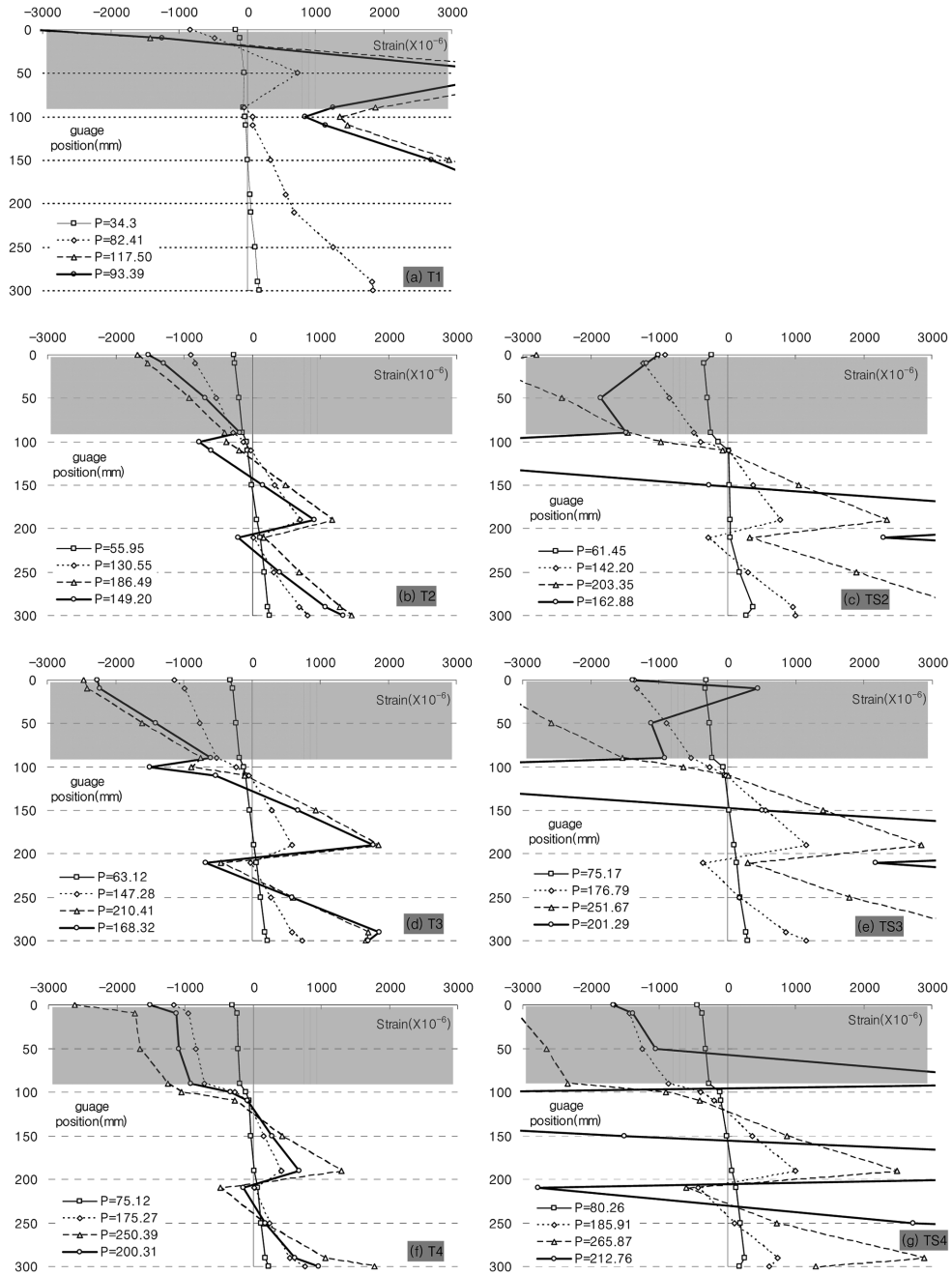


Fig. 13 Distribution of strain according to gauge position

maximum load and strength was lost thereafter, the upper and lower modules were separated before they reached 70% of the maximum load, and compression occurred at the top of the lower module. However, tension recurred at the maximum load. Subsequently, with the development of separation by a slip between modules, tensile strain increased simultaneously, and such increased tensile strain,

despite module separation, seems to be attributable to the mechanical adhesion due to the connecting bolt. Separation between modules appeared in all specimens except the T1 specimen, which is deemed to be due to shear failure of the bolt. It was found that transmission of force between modules occurred due to the shear strength from the bolt, the mechanical bond between the bolt and concrete, the chemical adhesion and the friction between the concrete and steel, etc. Also, with the increase in steel thickness, a proper shear connector should be necessarily used. Therefore, as soon as the steel thickness increases, the size or space of the bolt needs to be changed for shear connection between modules. Also, it is deemed that the behavior of TMPB should be clarified through further experiments with a shear connector as a parameter.

4.3.4 Analysis of shear strength

Shear strength per part is calculated as shown in Table 6. Shear strength was calculated in $V_c = \frac{1}{6} \sqrt{f_{ck}} b_w \cdot d$ for concrete, $V_s = \frac{f_y \cdot A_v \cdot d}{s}$ for stirrup, and $V_p = 0.6 F_y \cdot A_w$ for profile. Here, the f_y limit for stirrup was set to 400 MPa, V_s was calculated to not exceed 4 folds of V_c with 2-point loading and was compared with P/2 of support reaction. In general, for reinforced concrete slab and H-type steel composite beams, it is specified that shear strength shall be fully burden by steel, and in case of reinforced concrete-encased composite beams, the higher value shall be used between reinforced concrete and steel, and thus composite shear strength is not accepted. The T specimens without reinforcing stirrups were planned to not exceed shear strength V_1 when only with concrete or profile, but if two elements were to be combined, they were planned to exceed shear strength V_1 . The experiment showed that shear strength of all specimens exceeded that of concrete (V_c) but did not exceed shear strength (V_1) linked to the bending moment of the specimens. With regard to failure of the T-type specimens, which did not undergo shear reinforcement, except for the T1 specimen which underwent flexural failure, separation between modules and failure by a diagonal tension crack appeared, indicating that shear strength of the specimen did exceed that of concrete but shear strengths of steel could not be simply added up. Thus, studies need to be carried out to properly reflect the shear strength of steel and concrete for reasonable design. The TS specimens were designed to hold enough shear strength when only with concrete and stirrup but the experiment showed that they were broken by the compression failure of compressed concrete and the local buckling of compression steel due to decreased strength by separation between modules.

Table 6 Shear strength analysis

unit : kN

	V_c	V_s	$V_c + V_s$	V_p	$V_c + V_s + V_p$	$V_1 = \frac{P_{mt1}}{2}$	$V_2 = \frac{P_{mt2}}{2}$	$V_3 = \frac{P_{me}}{2}$
T1	46.6	-	46.6	37.4	84.0	59.7	47.08	58.8
T2	46.6	-	46.6	86.8	133.4	114.8	89.85	93.2
T3	46.6	-	46.6	127.8	174.4	150.0	108.64	105.2
T4	46.6	-	46.6	165.6	212.2	174.1	132.45	125.2
TS2	46.6	153.4	200.0	86.8	286.8	114.8	89.85	103.2
TS3	46.6	186.4	233.0	127.8	360.8	150.0	108.64	125.8
TS4	46.6	186.4	233.0	165.6	398.6	174.1	132.45	132.9

V_c : Shear force of concrete, V_s : Shear force of stirrup, V_p : Shear force of profile

5. Conclusion

The following conclusions were obtained from the experiment and theoretical analysis on the behavior of T-section modular composite profiled beams

- (1) In the T1 specimen, the whole section exhibited strain corresponding to yielding strain at least without separation between modules even without shear reinforcement because of the marginal difference in shear strength between the shear strength of the concrete section and that of the maximum bending moment. The section also underwent ductile behavior displaying the maximum strength similar to the theoretical value. Therefore, it is considered that the applicability of TMPB was sufficient, where profiles in proper thickness were used according to the scale of the specimen.
- (2) The ratios of theoretical maximum strengths to experimental strengths (P_{me} / P_{mt1}) of the TS specimens that underwent shear reinforcement were found to be higher than the T specimens respectively, and suitable shear reinforcing TMPB in the case where f_y is applied instead of f_{ye} , which exceeded the theoretical plastic bending moment (M_p).
- (3) The analysis on maximum shear strain of the side profile showed that in terms of the maximum load, the T specimens had 50% at least higher shear strain than the TS specimens with continuously increased shear strain, indicating that shear reinforcement prevents the decrease of bending moment in the case where the side profile receives shear force.
- (4) In all the specimens except the T1 specimen, separation between modules occurred, which is deemed to be due to the shear failure of the bolt. It is considered that the behavior of TMPB needs to be clarified by a bending experiment with a shear connector as a parameter.

Acknowledgment

“This work was supported by Basic Science Research Program through the National Research Foundation of Korea(NRF) funded by the Ministry of Education, Science and Technology(MEST)” (KRF-2008-313-D01148)

References

- ACI Committee 318 (2005), Building code requirement for structural concrete (318-05) and Commentary (318R-05) American Concrete Institute.
- Ahmed, M., Oehlers, D.J. and Bradford, M.A. (2000), “Retrofitting reinforced concrete beams by bolting steel plates to their sides. Part 1: Behavior and experiments,” *Struct. Eng. Mech.*, **10**(3), 211-226.
- Bencardino, F., Spadea, G and Swamy, R.N. (2002), “Strength and ductility of reinforced concrete beams externally reinforced with carbon fiber fabric,” *ACI Struct. J.*, **99**(2), 163-171
- Brian Uy and Andrew Bradford (1995), “Ductility of profile beams. Part I: Experimental study,” *J. Struct. Eng-ASCE*, **121**(5), 876-882.
- Brian Uy and Andrew Bradford (1995), “Ductility of profile beams. Part II: Analytical study,” *J. Struct. Eng-ASCE*, **121**(5), 883-889.
- Hyung-Joon Ahn and Soo-Hyun Ryu (2007), “Experimental study on flexural strength of modular composite profile beams,” *Steel. Compos. Struct.*, **7**(1), 71-85.
- Hyung-Joon Ahn and Soo-Hyun Ryu (2008), “Experimental study on flexural strength of reinforced modular composite profiled beams,” *Steel. Compos. Struct.*, **8**(4), 313-328.
- Minglan Peng and Zhifei Shi (2004), “Interface characteristics of RC beams strengthened with FRP plate struct,”

- Struct. Eng. Mech.*, **18**(3), 315-330.
- Oehlers D.J. (1993), "Composite profile beams," *J. Struct. Eng-ASCE*, **119**(4), 1085-1100.
- Oehlers D.J., Wright H.D. and Burnet M.J. (1994), "Flexural strength of profile beams," *J. Struct. Eng-ASCE*, **120**(2), 378-393.
- Oehlers, D.J., Ahmed, M., Nguyen N.T. and Bradford, M.A.(1997), "Transverse and longitudinal partial interaction in composite bolted side-plated reinforced concrete beams," *Struct. Eng. Mech.*, **5**(5), 553-563.
- Oehlers, D.J., Ninh T Nguyen and Bradford, M.A. (2000), "Retrofitting by adhesive bonding steel plates to sides of R.C. beams. Part 1: Debonding of plates due to flexure," *Struct. Eng. Mech.*, **9**(5), 491-503.
- Oehlers, D.J., Ninh T Nguyen and Bradford, M.A. (2000), "Retrofitting by adhesive bonding steel plates to sides of R.C. beams. Part 2: Debonding of plates due to shear and design rules," *Struct. Eng. Mech.*, **9**(5), 505-518.
- Oehlers, D.J., Ahmed, M., Nguyen N.T. and Bradford, M.A. (2000), "Retrofitting reinforced concrete beams by bolting steel plates to their sides. Part 2: Transverse interaction and rigid plastic design," *Struct. Eng. Mech.*, **10**(3), 227-243.
- Sang Hun Kim and Riyad S. Aboutaha, (2004), "Ductility of carbon fiber-reinforced polymer (CFRP) strengthened reinforced concrete beams: Experimental investigation," *Steel. Compos. Struct.*, **4**(5), 333-353.

CC